

Investigation of flame structure in plasma-assisted turbulent premixed methane-air flame

Hualei ZHANG (张华磊), Liming HE (何立明), Jinlu YU (于锦禄),
Wentao QI (祁文涛) and Gaocheng CHEN (陈高成)

Science and Technology on Plasma Dynamics Lab, Air Force Engineering University, Xi'an 710038,
People's Republic of China

E-mail: 1129025832@qq.com

Received 20 June 2017, revised 2 November 2017

Accepted for publication 6 November 2017

Published 12 December 2017



CrossMark

Abstract

The mechanism of plasma-assisted combustion at increasing discharge voltage is investigated in detail at two distinctive system schemes (pretreatment of reactants and direct *in situ* discharge). OH-planar laser-induced fluorescence (PLIF) technique is used to diagnose the turbulent structure methane-air flame, and the experimental apparatus consists of dump burner, plasma-generating system, gas supply system and OH-PLIF system. Results have shown that the effect of pretreatment of reactants on flame can be categorized into three regimes: regime I for voltage lower than 6.6 kV; regime II for voltage between 6.6 and 11.1 kV; and regime III for voltage between 11.1 and 12.5 kV. In regime I, aerodynamic effect and slower oxidation of higher hydrocarbons generated around the inner electrode tip plays a dominate role, while in regime III, the temperature rising effect will probably superimpose on the chemical effect and amplify it. For wire-cylinder dielectric barrier discharge reactor with spatially uneven electric field, the amount of radicals and hydrocarbons are decreased monotonically in radial direction which affects the flame shape. With regard to *in situ* plasma discharge in flames, the discharge pattern changes from streamer type to glow type. Compared with the case of reactants pretreatment, the flame propagates further in the upstream direction. In the discharge region, the OH intensity is highest for *in situ* plasma assisted combustion, indicating that the plasma energy is coupled into flame reaction zone.

Keywords: plasma assisted combustion, laser-induced fluorescence, flame structure, turbulent premixed combustion, dump burner

(Some figures may appear in colour only in the online journal)

1. Introduction

Increasing attention has been paid to plasma-assisted combustion in the last few decades owing to its promising effects on the reliable ignition and stable combustion. The relevant research has evolved from qualitative descriptions to quantitative analyses, from the experimental phenomenon to multi-scale simulation, from individual plasma-assisted method to multiple methods, from low speed to high speed and from low frequency discharge to high frequency discharge and so on [1–7]. The underlying mechanisms are ascribed to the following three effects [8, 9]: (1) temperature rising effect induced

by joule heating, (2) chemical effect induced by active radicals, (3) aerodynamic effect induced by the transport of charged particles and newly generated species as well as the shock waves and gas expansion generated by the fast heating of the gas. The time and length scales vary from nanosecond to second and nanometer to meter in plasma-assisted combustion, respectively [10]. Plasma, flow, and heat and mass transfer are highly coupled. Additionally, it is difficult to get homogeneous discharges at atmospheric or higher pressure and the fundamental chemistry is also a challenge. Thus, the study on plasma-assisted combustion is extremely sophisticated and the mechanisms remain unclear up to date.

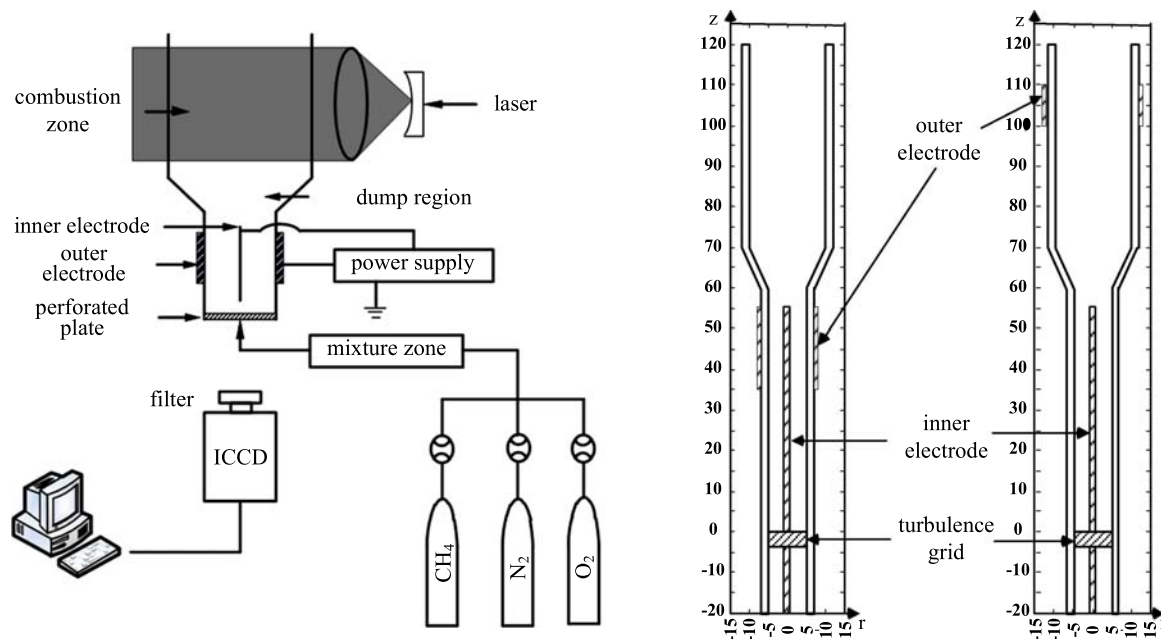


Figure 1. Schematic of plasma-assisted turbulent premixed flame system.

Combustion mainly involves four scientific disciplines: thermodynamics, chemical kinetics, fluid mechanics, and transport phenomena [11]. Therefore, combustion performance can be improved through aforementioned disciplines. Plasma-assisted combustion can affect all the four scientific disciplines so that plasma has notable effects on combustion. According to which species the plasma energy is coupled into, plasma-assisted combustion can be classified into the following four approaches: the discharge in oxidizer, fuel, mixtures and the fuel addition such as water. In terms of the moment that plasma energy exerts, plasma-assisted combustion can be classified into pretreatment of reactants [12–15], direct *in situ* plasma discharges [16] and after-treatment of combustion [17]. Studies have devoted extensive efforts toward the pretreatment of reactants and after-treatment of combustion. Nevertheless, the effect of direct *in situ* discharges on the flame is not well investigated and the plasma-flame interaction is far from understood. In addition, the differences between the different methods are not compared in the previous studies. On the one hand, the plasma and flame are coupled in the method of *in situ* plasma discharges while decoupled in the other two methods. On the other hand, the main characteristics of flame are high temperature, visible and pre-ionized and the discharge pattern may change, compared with the other methods. Therefore, further researches on plasma-assisted combustion are still needed.

In this paper, an experimental system is established to study the effect of pretreatment of reactants and *in situ* plasma discharges on the premixed methane-air flame. In order to get a better understanding of the mechanism of plasma-assisted combustion, the distribution of hydroxyl radical in its fundamental state (OH) is diagnosed by planar laser-induced fluorescence (PLIF) technique.

2. Experimental setup and diagnostic methods

A fundamental experimental system has been designed to study the plasma-assisted combustion, featuring convenient measurements. The blow-off velocity of the nozzle-type Bunsen burner without pilot flame is about 2 m s^{-1} , which is too small to study the plasma-assisted combustion. Therefore, a dump burner is established as shown in figure 1, and the mean velocity of burner inlet can range from 0 to 15 m s^{-1} . In the dump region, a recirculation zone is formed which provides flame stabilization.

The experimental apparatus consists of dump burner, plasma-generating system, gas supply system and OH-PLIF system, as shown in figure 1. The inner diameter of burner inlet is 10 mm and the outer diameter is 14 mm. The inner and outer diameter of burner outlet are 20 mm and 24 mm, respectively. The uniform turbulence is generated by a perforated plate ($-4 \text{ mm} < z < 0 \text{ mm}$, $\text{const } \varnothing = 10 \text{ mm}$) with the orifice diameter of 1.6 mm, opening ratio of 48.64% and thickness of 4 mm. The other sizes of burner are presented in figure 1. The plasma-generating system consists of a wire-cylinder reactor and an AC double high voltage difference power (CTP-2000S, Suman Electronics). The two outputs of the power supply are high voltage but the phase difference is 180° . The frequency of power supply is set as 10 kHz. The inner electrode is made of tungsten needles with 1.6 mm diameter, which has excellent high temperature resistance and electronic emission ability. The outer electrode is made of a woven stainless steel mesh. The inner and outer electrode location can be adjusted. The flow rate is adjusted by MKS mass flow controllers and the methane and air are mixed in a stainless steel chamber before entering the burner.

The discharge voltage and current are measured with Tektronix P6015A (1000:1) high voltage probe and Tektronix TCP0030 current probe (1:1 for measurement range 5 A and

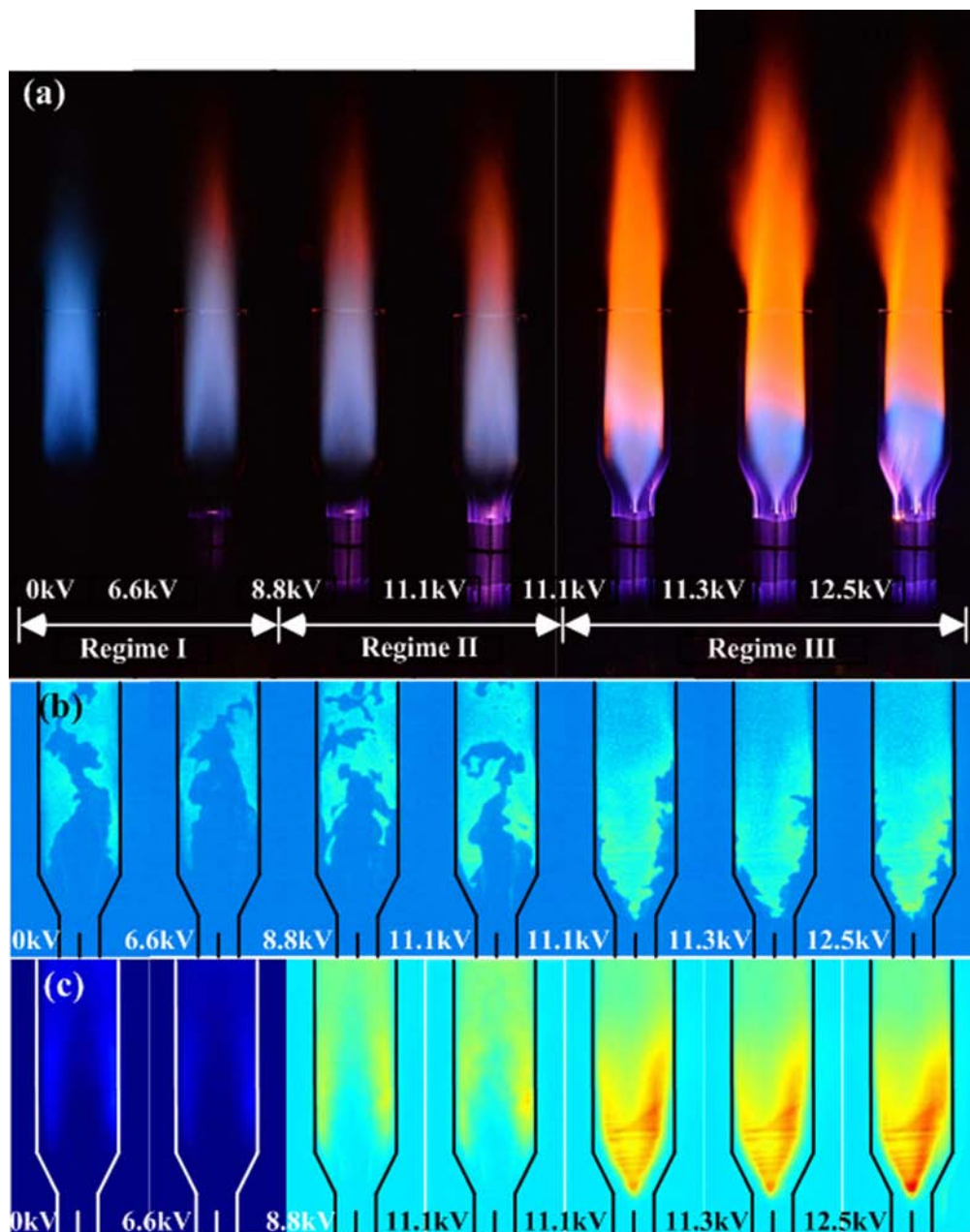


Figure 2. Direct and OH-PLIF image of plasma-assisted turbulent premixed flame: (a) images for turbulent CH_4 -air premixed flame with the equivalence ratio of 0.9; (b) single 2D OH-PLIF images as a function of increasing voltage; (c) average 2D OH-PLIF images as a function of increasing voltage.

10:1 for measurement 30 A; the bandwidth is 120 MHz) and recorded via an oscilloscope (Tektronix DPO4104B). The direct flame images are captured by a digital camera (Nikon D5200). The OH-PLIF system uses Nd:YAG laser (Quanta-Ray Pro-190) with a wavelength of 355 nm and a pumped dye laser (Sirah PRSC-G-3000) with a frequency doubler as the laser source. The pulse energy is about 8 mJ. The Q1(8) transition of the $\text{A}^2\Sigma \leftarrow \text{X}^2\Pi(1, 0)$ line of OH radical is excited with the wavelength of 282.769 nm. The OH signals are detected by an ICCD camera (La Vision Image Prox) with 10 Hz sampling frequency synchronized with the laser. The resolution of the OH-PLIF system is 1600×1200 pixels with

$136 \mu\text{m}/\text{pixel}$. 200 images are taken to obtain the dynamic characteristics of the turbulent premixed flame.

In this paper, the outer electrode is located respectively at $35 \text{ mm} < z < 55 \text{ mm}$ with constant $\varnothing = 14 \text{ mm}$ in section 3.1 and $100 \text{ mm} < z < 110 \text{ mm}$ with constant $\varnothing = 24 \text{ mm}$ in section 3.2 to investigate the effect of pre-treatment of reactants and direct *in situ* plasma discharges on the turbulent flame. The inner electrode is located at $-20 \text{ mm} < z < 55 \text{ mm}$ with constant $\varnothing = 10 \text{ mm}$ and is fixed in the experiment. The equivalence ratio is fixed at 0.9 (the mass flow rates of methane, nitrogen and oxygen are 4.0671 min^{-1} , 23.781 min^{-1} , and 9.041 min^{-1} (1 bar, 298 K),

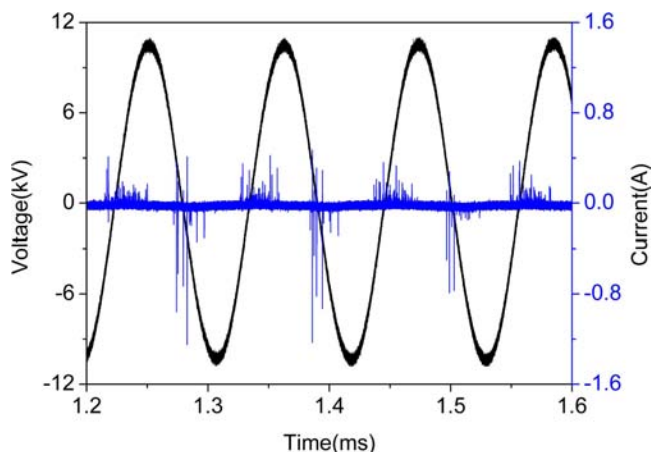


Figure 3. Electrical waveforms for $V = 11.1$ kV.

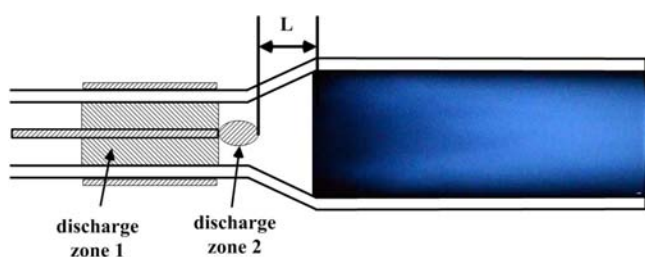


Figure 4. Schematic interpretation for different discharge zones.

respectively) and the mean velocity is 10 m s^{-1} in the burner inlet.

3. Results and discussion

3.1. Effect of pretreatment of reactants on flame

Figure 2 shows the direct flame images and the single and average 2D OH-PLIF images under various voltage levels. The OH-PLIF and the direct images are taken from the opposite sides of the burner. A typical premixed flame is stabilized in the dump region (voltage 0.0 kV). A light blue hue is observed as a result of CH^* emission [18]. Based on the flame luminosities and the flame shapes under different applied voltage, the plasma-assisted turbulent premixed can be categorized into three regimes: regime I for voltage lower than 6.6 kV; regime II for voltage between 6.6 and 11.1 kV; and regime III for voltage between 11.1 and 12.5 kV.

In regime I, as voltage increases, the flame is longer, darker and emissive. The color becomes red at the downstream and the OH intensity gets lower. Strong discharge occurs around the inner electrode tip. In regime II, the flame becomes even darker and emissive in the flame tip, the flame front becomes wrinkled and fluctuates seriously, and the OH intensity gets higher. The discharge volume around the tip of the inner electrode increase and the luminosities become stronger. The minimum distance between the discharge and flame is closer. At about 7 s after the plasma initiation at voltage of 11.1 kV, the flame shape transfers from regime II to regime III. In regime III, V-shaped flame is formed and

comprised by two parts: a short blue flame and a long yellow flame. A discharge channel is established between the flame and the tip of the inner electrode. From figure 2(c), it could be seen that the OH intensity is asymmetric. This is mainly because the inner electrode is not in the center of the tube perfectly. The OH is mainly distributed in the dump region and downstream of the burner. It is worth noting that OH intensity is low between the tip of the inner electrode and the dump region.

The typical electrical waveforms for $V = 11.1$ kV is shown in figure 3. From the waveforms, we know that dielectric barrier discharge (DBD) discharge is streamer discharge which is characterized by numerous current pulses which is called micro-discharge channels distributed in space and time randomly. The discharge current in the positive half cycle of the applied voltage is more uniform than that of the negative half cycle.

For wire-cylinder DBD discharge with nonuniform electrode field [19] (especially the wire electrode is bare and used as high voltage electrode), discharge occurs at the tip of the inner electrode. Therefore, the discharge zone has been divided into two zones (plasma zone 1: region between the inner and outer electrode; plasma zone 2: around the tip of the inner electrode) as shown in figure 4.

In regime I, as the applied voltage is low, the discharge in plasma zone 1 is very weak and the temperature rising effect can be negligible. Although the applied voltage is low, the electric field at the tip of the inner electrode is high enough to form corona discharge and its lighting emission zone is confined around the inner electrode (plasma zone 2). As mentioned by Vincent-Randonnier *et al* [20], discharge in the methane can yield higher (C_2 – C_5 , or even higher) hydrocarbons including saturated and unsaturated hydrocarbon and radicals (CH_3 , O). The electric field at the inner electrode tip is capable of generating higher hydrocarbons and radicals, thus higher hydrocarbons and radicals are formed around the inner electrode tip. However, the oxidation of higher hydrocarbons is slower and higher hydrocarbons have lower sooting limits, especially C_2H_2 is prone to form soot. Therefore, the flame becomes darker and the color becomes red as a result of soot radiation. In regime II and III, high voltage increases the amount of hydrocarbons, so the radiation of soot gets stronger and the flame color turns to yellow.

In regime II, as the voltage increases, the discharge power increases and more radical and active species are generated. Additionally, the premixed methane-air is heated by the discharge energy. As a result, the combustion is enhanced and the OH intensity increases. In this regime, the three effects of the plasma-assisted combustion are highly coupled and that dominated effect cannot be picked out. The distance between the flame and the plasma zone 2 as indicated by L in figure 4 becomes shorter. At the voltage of 11.1 kV, at about 7 s later after the observation start, the inner electrode is affected by the joule heating and the heat conducted from the flame which results in a stronger discharge. Finally, the flame shape transfers from regime II to regime III.

In the regime III, as the voltage increases, L becomes shorter enough, so a discharge channel is formed between the

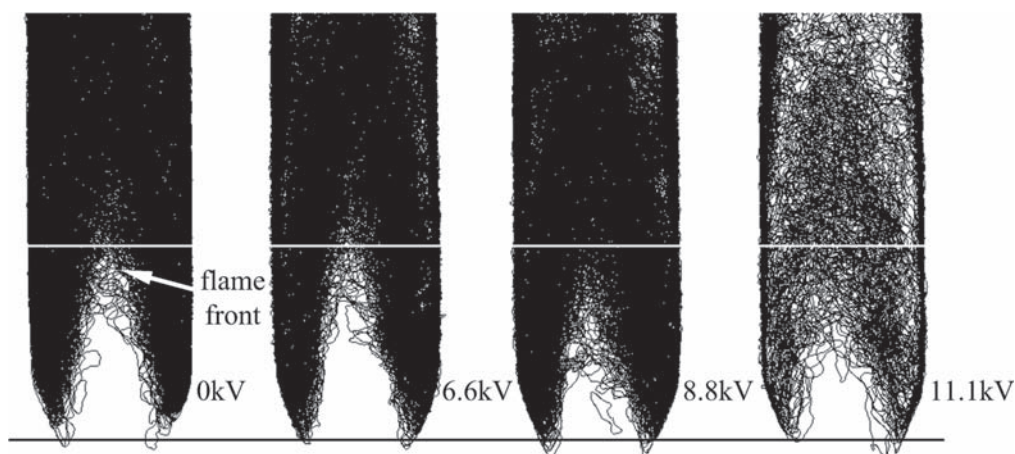


Figure 5. Flame front or turbulent CH₄-air premixed flame.

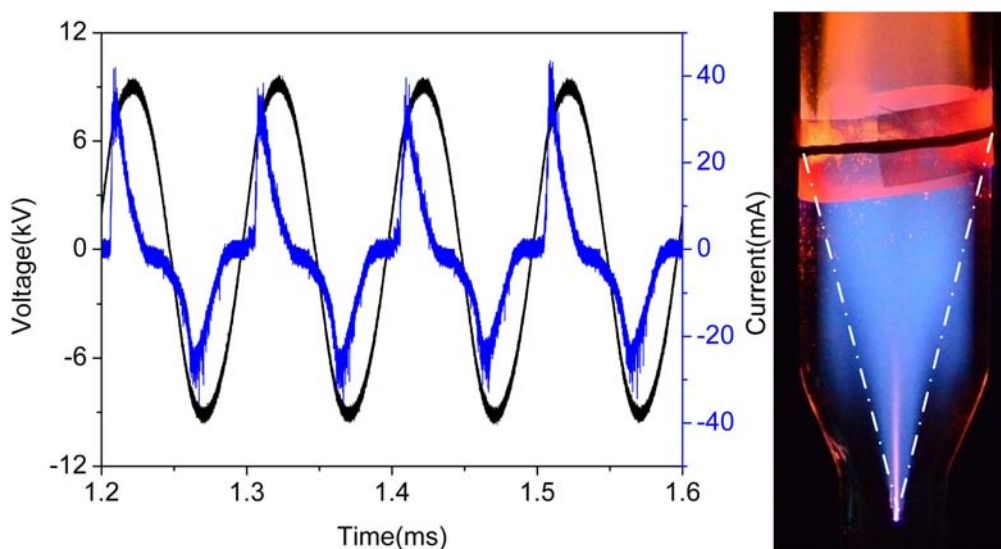


Figure 6. Typical electrical waveforms of *in situ* plasma discharge (left: electrical waveforms; right: flame image).

flame and the inner electrode, meanwhile expanding in the downstream and the discharge between the inner and the outer electrodes becomes weaker which is similar to the phenomenon investigated by Vincent-Randonnier *et al* [3]. When the discharge reaches the flame region, the high local temperature leads to a low density of the gas and an increase of the electron free mean path, thus facilitating progression of the discharge, so the flame can serve an extend electrode which is resistive [16, 21]. As a result, the discharge in zone 1 becomes weaker where discharge occurs at room temperature. Compared with the flame shape without plasma, the blue part of the flame is shorter as a portion of methane is reformed into higher hydrocarbons and radicals. The oxidation rate of different higher hydrocarbons varies, so the structure of flame is layered. In this regime, the temperature rising effect will probably superimpose on the chemical effect and amplify it.

To get a better understanding of the turbulent front, the flame front is determined through binarizing with a threshold value, and 200 images are used at various voltages except for 11.1 kV (75 images) as shown in figure 5. In regime I, there is

no obvious change in the flame front. In regime II, the flame front moves upstream (*Z*-direction) and the cone angle of the flame front increases with voltage. This indicates the flame propagation speed becomes higher.

3.2. Effect of *in situ* plasma discharge on premixed flame

Typical electrical waveforms and discharge image are shown in figure 6. In our experiment, the outer electrode is covered with quartz and the discharge system belongs to DBD. In most cases, DBDs are streamer discharge which is similar to the discharge in section 3.1. Nevertheless, from the waveforms, there are only two pulsed currents with opposite polarity per cycle of the applied voltage in this section. The peak discharge voltage is about 9.3 kV and the peak current is about 40 mA, which is different from the streamer discharge and the arc discharge with the characteristics of low voltage and high current. The discharge is more like glow discharge which is also found by Lacoste *et al* [22]. There exist two typical discharge instabilities [23]: one is vanish of charged

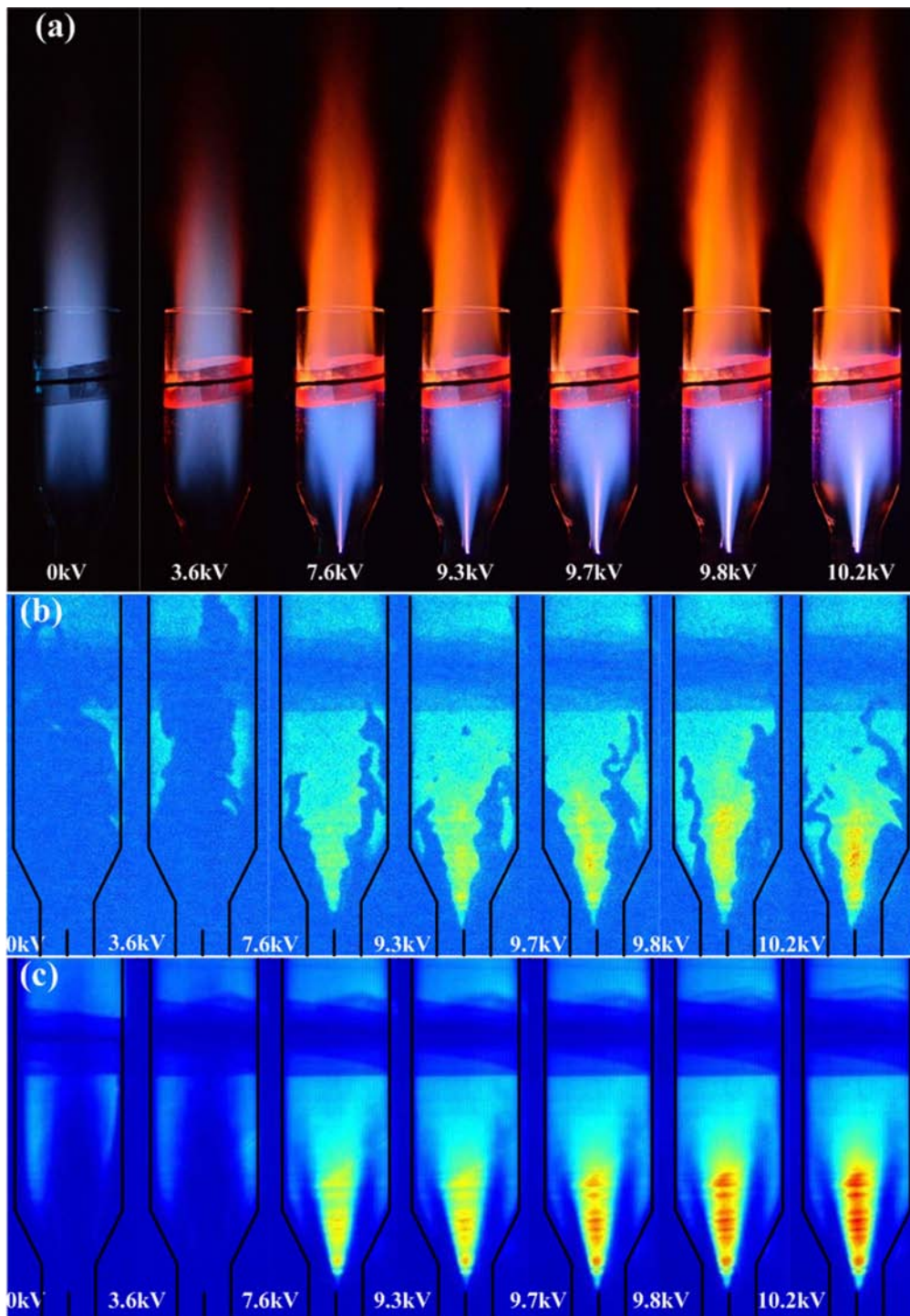


Figure 7. Direct and OH-PLIF image of plasma-assisted turbulent premixed flame: (a) images for turbulent CH₄-air premixed flame with the equivalence ratio of 0.9; (b) single 2D OH-PLIF images as a function of increasing voltage; (c) average 2D OH-PLIF images as a function of increasing voltage.

particles due to the electronegative gas such as O₂ and the other is the decrease of neutral particles which is called thermal instabilities. In the flame, the density is low and the reduced field intensity is high, which means that the mean free path of electrons increases and the electrons can gain more energy from the electric field. In addition to that, there are abundant free electrons and concentration of electronegative gas such as O₂ is low in the flame. These factors

suppress the discharge instabilities and promote the formation of glow discharge.

Figure 7 shows the direct flame images and the single and average 2D OH-PLIF images under various voltages. The flame exhibits M shape structure as the discharge voltage increases. The discharge channel color varies from purple to white, with increasing light intensity and discharge area. In the discharge region, the OH intensity is highest for *in situ*

plasma assisted combustion while OH intensity is low for pretreatment of reactants. That indicates there is no flame in the discharge zone in section 3.1 and the plasma in the discharge zone only generates hydrocarbons and radicals. Discharge zone is the region where the fuel burns vigorously, indicating that the plasma energy is coupled into the reaction zone of the flame and facilitates enhancement of flame.

It is interesting to note that the dot dash line between inner and outer electrodes in the right image of figure 6 is part of the boundary of the M shape flame. Compared with the flame without plasma, the difference of flame shape lies in the center. The reason is as follows. The intensity of the discharge is strongest around the centerline and gradually decreases along the radial direction. Therefore, the flame shape at the two sides of the burner is the same with the combustion without plasma and a V-shaped flame is formed around the centerline.

From figure 7, with the increasing of voltage, the flame in the discharge zone is blue and is yellow at the downstream. The reason is the same with section 3.1 for the yellow flame. Compared with the case of reactants pretreatment, the flame propagates further in the upstream direction. It indicates that the turbulent flame speed has gained seriously. As mentioned by Lacoste *et al* [24], the thermal impact of glow discharge is negligible and chemical effect of the mixture seems to be the realistic explanation of the plasma effect. In the figures 7(b) and (c), the average intensity of the OH increases with the increase of the discharge voltage. The OH intensity of the OH along the axes is discontinues and can be clearly seen from figure 7(c). That may be due to the periodic discharge coupled with the air flow and ionic wind.

4. Conclusions

The effect of pretreatment of reactants and *in situ* plasma discharge on turbulent premixed methane-air flame is studied and the flame structure is characterized with OH-PLIF system.

The effect of pretreatment of reactants on flame can be categorized into three regimes: regime I for voltage lower than 6.6 kV; regime II for voltage between 6.6 and 11.1 kV; and regime III for voltage between 11.1 and 12.5 kV. In regime I, as voltage increases, the flame is longer, darker and emissive. The color becomes red at the downstream and the OH intensity gets lower. Aerodynamic effects and slower oxidation of the high hydrocarbons generated around the inner electrode tip dominate in this regime. In regime II, the flame becomes even darker and emissive in the flame tip, the flame front becomes wrinkled and fluctuates more severely with higher OH intensity. The three effects of the plasma-assisted combustion are highly coupled and the dominated effect cannot be picked out. In regime III, the V-shaped flame is comprised by a short blue flame and a long yellow flame and the flame luminosity increase. A discharge channel is established between the flame and the tip of the inner electrode. The mechanism that the temperature rising

effect will probably superimpose on the chemical effect and amplify it dominates in this regime.

In the investigation of *in situ* plasma discharge on flame, the discharge pattern changes from streamer type to glow discharge. Compared with the case of reactants pretreatment, the flame propagates further in the upstream direction. In the discharge region, the OH intensity is highest for *in situ* plasma assisted combustion, indicating that the plasma energy is coupled into flame reaction zone.

Further experiments such as CH* emission imaging and velocity fields measurements are needed to investigate the interaction among plasma, flame and flow.

Acknowledgments

This work was financed by National Natural Science Foundation of China (No. 51436008). Hualei Zhang would like to thank Dr Jinhua Wang and Meng Zhang for many helpful discussions on various aspects of turbulent flame structure and assistance in OH-PLIF measurement.

References

- [1] Starikoovskiy A Y 2005 *Proc. Combust. Inst.* **30** 2405
- [2] Ju Y G and Sun W T 2015 *Prog. Energy Combust. Sci.* **48** 21
- [3] Vincent-Randonnier A *et al* 2007 *Plasma Sources Sci. Technol.* **16** 149
- [4] Wang C J and Wu W 2014 *Combust. Flame* **161** 2073
- [5] Firsov A A, Shurupov M A and Yarantsev D A 2014 Plasma-assisted combustion in supersonic airflow: optimization of electrical discharge geometry *52nd Aerospace Sciences Meeting (National Harbor, Maryland, 13–17 January 2014)* (America: AIAA) AIAA paper, 2014-0988 (<https://doi.org/10.2514/6.2014-0988>)
- [6] Lacoste D A *et al* 2013 *Proc. Combust. Inst.* **34** 3259
- [7] Nagaraja S 2014 Multi-scale modeling of nanosecond plasma assisted combustion *PhD Thesis* Georgia Institute of Technology (<http://hdl.handle.net/1853/52228>)
- [8] Vu T M *et al* 2014 *Combust. Flame* **161** 917
- [9] Xu D A *et al* 2014 *J. Phys. D: Appl. Phys.* **47** 235202
- [10] <http://publish.illinois.edu/exascale-plasma>
- [11] Law C K 2006 *Combustion Physics* (New York: Cambridge University Press)
- [12] Lee D H *et al* 2007 *Proc. Combust. Inst.* **31** 3343
- [13] Lee D H *et al* 2010 *Int. J. Hydrogen Energy* **35** 4668
- [14] Wu W, Fuh C A and Wang C J 2015 *Combust. Sci. Technol.* **187** 999
- [15] Hemawan K W *et al* 2006 *Appl. Phys. Lett.* **89** 141501
- [16] Cha M S *et al* 2005 *Combust. Flame* **141** 438
- [17] Cha M S *et al* 2007 *Int. J. Plasma Environ. Sci. Technol.* **1** 28
- [18] Gaydon A G 1974 *The Spectroscopy of Flames* (London: Chapman and Hall) (<https://doi.org/10.1007/978-94-009-5720-6>)
- [19] Fang Z *et al* 2008 *J. Electrostat.* **66** 421
- [20] Vincent-Randonnier A *et al* 2007 *IEEE Trans. Plasma Sci.* **35** 223
- [21] Han S U 1999 *Phys. Plasmas* **6** 4366
- [22] Lacoste D A *et al* 2017 *Prog. Combust. Inst.* **36** 4145
- [23] Raizer Y P 1993 *Gas Discharge Physics* (Berlin: Springer)
- [24] Lacoste D A *et al* 2017 *Combust. Sci. Technol.* **189** 2012